Title

Rheumatoid Arthritis Exacerbates the Severity of Osteonecrosis of the Jaws (ONJ) in Mice. A Randomized, Prospective, Controlled Animal Study

Journal

Journal of Bone and Mineral Research, 31(8)

ISSN

0884-0431

Authors

de Molon, Rafael Scaf
Hsu, Chingyun
Bezouglaia, Olga
et al.

Publication Date

2016-08-01

DOI

10.1002/jbmr.2827

Peer reviewed

HHS Public Access

Author manuscript

J Bone Miner Res. Author manuscript; available in PMC 2017 August 01.

Published in final edited form as:

J Bone Miner Res. 2016 August ; 31(8): 1596–1607. doi:10.1002/jbmr.2827.

Rheumatoid arthritis exacerbates the severity of osteonecrosis of the jaws (ONJ) in mice. A randomized, prospective, controlled animal study

Rafael Scaf de Molon[1,2], **Chingyun Hsu**[1], **Olga Bezouglaia**[1], **Sarah M. Dry**[3], **Flavia Q. Pirih**[4], **Akrivoula Soundia**[1], **Fernando Queiroz Cunha**[5], **Joni Augusto Cirelli**[2], **Tara L. Aghaloo**[1,*], and **Sotirios Tetradis**[1,6,*]

[1]Division of Diagnostic and Surgical Sciences, UCLA School of Dentistry, Los Angeles, CA 90095, USA

[2]Department of Diagnosis and Surgery, School of Dentistry at Araraquara, Sao Paulo State University, Araraquara 14801–903, Brazil

[3]Department of Pathology and Laboratory Medicine, David Geffen School of Medicine at UCLA, Los Angeles, CA 90095, USA

[4]Division of Constitutive & Regenerative Sciences, UCLA School of Dentistry, Los Angeles, CA 90095, USA

[5]Department of Pharmacology, School of Medicine of Ribeirao Preto, Sao Paulo 14049, Brazil

[6]Molecular Biology Institute, UCLA, Los Angeles, CA 90095, USA

Abstract

Rheumatoid arthritis (RA), an autoimmune inflammatory disorder, results in persistent synovitis with severe bone and cartilage destruction. Bisphosphonates (BPs) are often utilized in RA patients to reduce bone destruction and manage osteoporosis. However, BPs, especially at high doses, are associated with osteonecrosis of the jaw (ONJ). Here, utilizing previously published ONJ animal models, we are exploring interactions between RA and ONJ incidence and severity. DBA1/J-mice were divided in 4 groups: control, zoledronic acid (ZA), collagen induced arthritis (CIA), and CIA-ZA. Animals were pre-treated with vehicle or ZA. Bovine collagen II emulsified in Freund's adjuvant was injected to induce arthritis (CIA) and the mandibular molar crowns were drilled to induce periapical disease. Vehicle or ZA treatment continued for 8-weeks. ONJ indices

*Corresponding Authors Sotirios Tetradis DDS, PhD, UCLA School of Dentistry, 10833 Le Conte Ave. CHS Rm. 53-068, Los Angeles, CA 90095-1668, Tel: (310) 825-5712, Fax: (310) 825-7232 stetradis@dentistry.ucla.edu. Tara L. Aghaloo DDS, MD, PhD, UCLA School of Dentistry, 10833 Le Conte Ave. CHS Rm. 53-009, Los Angeles, CA 90095-1668, Tel: (310) 794-7070, Fax: (310) 825-7232, taghaloo@dentistry.ucla.edu.

CONFLICT OF INTEREST

All authors state that they do not have any conflicts of interest regarding this manuscript.

AUTHOR CONTRIBUTIONS

Study conception and design. RSM, CH, OB, SMD, FQP, AS, FQC, JAC, TLA, and ST; Acquisition of data. RSM, CH, OB, SMD, FQP, AS, FQC, JAC, TLA, and ST; Analysis and interpretation of data. RSM, SMD, JAC, TLA, and ST; Edition of the manuscript: RSM, CH, OB, SMD, FQP, AS, FQC, JAC, TLA, and ST; Drafted the manuscript: RSM and ST. All authors were involved in revising the paper critically for important intellectual content, and all authors approved the final version to be published. RSM and ST had full access to all of the data in the study and take responsibility for the integrity of the data and the accuracy of the data analysis.

were measured by micro-CT and histological examination of maxillae and mandibles. Arthritis development was assessed by visual scoring of paw swelling, and by micro-CT and histology of interphalangeal and knee joints. Maxillae and mandibles of control and CIA mice showed bone loss, PDL space widening, lamina dura loss and cortex thinning. ZA prevented theses changes in both ZA and CIA-ZA groups. Epithelial to alveolar crest distance was increased in the control and CIA mice. This distance was preserved in ZA and CIA-ZA animals. Empty osteocytic lacunae and areas of osteonecrosis were present in ZA and CIA-ZA but more extensively in CIA-ZA animals, indicating more severe ONJ. CIA and CIA-ZA groups developed severe arthritis in the paws and knees. Interphalangeal and knee joints of CIA mice showed advanced bone destruction with cortical erosions and trabecular bone loss, and ZA treatment reduced these effects. Importantly, no osteonecrosis was noted adjacent to areas of articular inflammation in CIA-ZA mice. Our data suggest that ONJ burden was more pronounced in ZA treated CIA mice and that RA could be a risk factor for ONJ development.

Keywords

Collagen-induced arthritis; rheumatoid arthritis; osteonecrosis of the jaws; bisphosphonates; ONJ; osteoclasts; antiresorptive

INTRODUCTION

Rheumatoid arthritis (RA), an immunologically driven long-term disorder is characterized by persistent synovitis, systemic inflammation, and presence of autoantibodies (particularly to rheumatoid factor and citrullinated peptide), leading to long-term joint damage, chronic pain, loss of function and disability.[1,2] An exacerbated immune response from the activation of immune, inflammatory and resident cells is responsible for most of the tissue damage observed in RA, while osteoclastic activation plays major role in joint destruction.[3,4] Several treatments for RA have been developed and include nonsteroidal anti-inflammatory drugs (NSAIDs), corticosteroids, disease-modifying antirheumatic drugs (DMARDs), biologic agents (tumor necrosis factor or interleukin inhibitors) and JAK inhibitors.[1,5] All treatment strategies aim to reduce periarticular inflammation and limit joint destruction.

A major comorbidity in RA patients is a generalized skeletal BMD reduction and micro architectural deterioration.[6–8] RA vs. non-RA patients, show a 22.1 % increased incidence of osteoporosis and 11.4 % BMD reduction, while the overall frequency of osteoporosis and BMD below the expected age range in RA vs. non-RA subjects was 1.9 and 7.8 times higher, respectively.[9]

Nitrogen-containing bisphosphonates (BPs) strong inhibitors of osteoclastic bone resorption, are widely used to manage bone diseases, such as osteoporosis[10] or bone malignancy.[11] Many patients with RA are treated with bisphosphonates for managing their osteoporosis. Furthermore, the beneficial effects of BPs in the RA mediated focal osteolysis have been shown.[12–14] Indeed, BPs are among the most frequent prescribed drugs in rheumatologic practice.[15,16]

An infrequent but serious adverse effect of BPs is osteonecrosis of the jaw (ONJ) especially during intravenous high dose administration.[17] ONJ is defined as an area of exposed bone or bone that can be probed through an intraoral fistula in the maxillofacial region that does not heal within 8 weeks in patients exposed to antiresorptive medications and without history of radiation therapy to the jaws.[18,19] ONJ is most frequently observed after dental interventions such as tooth extraction, periodontal disease and in patients receiving corticosteroid treatment.[18,20,21] Recently, the term medication-related ONJ (MRONJ) was proposed[21] to include ONJ cases related to antiangiogenic therapies.

Despite described in 2004, pathophysiology of ONJ remains largely unknown.[22] Parameters that increase the risk for ONJ include dose and duration of antiresorptives, dentoalveolar surgery, concomitant dental disease, corticosteroid and anti-angiogenic treatment, and diabetes.[23–26] Interestingly, clinical studies point to an increased incidence of ONJ in RA patients and suggest that RA may represent a significant risk factor for the development of ONJ when BPs are administered to manage osseous complications.[8,20,27–29] However, the validity of this conclusion has been questioned, since almost all patients were receiving steroids, DMARDs, or a combination of these immunosuppressive agents that could alone increase ONJ risk.[28] Experimental data that directly explore the incidence and severity of ONJ in the absence or presence of RA are lacking.

Here, we employed two previously published ONJ mouse models utilizing either experimental periapical disease of mandibular teeth or naturally occurring periradicular inflammation of maxillary teeth [30–33] with a well-established model of collagen-induced arthritis (CIA) to explore the interplay between RA and ONJ. Our findings indicate that, jaw osteonecrosis was more extensive in ZA treated CIA mice in both maxilla and mandible, suggesting that systemic inflammation in RA compounds ONJ severity. ZA reduced bone resorption and cartilage destruction but not synovial inflammation in the hind paws and knee joints. Importantly, no osteonecrosis was noted adjacent to areas of articular inflammation in ZA treated mice with CIA.

MATERIALS AND METHODS

Animal care

Mice and surgical procedures were handled according to the guidelines of the Institutional Animal Care and Use Committee of UCLA. 10-week old DBA1/J male mice (Jackson Laboratories, Bar Harbor, ME, USA) were randomly divided into four experimental groups of 6 animals each: control (vehicle), ZA, CIA and CIA-ZA. Animals were pre-treated with *i.p.* injections of endotoxin free saline (vehicle) or 200 μg/kg zoledronic acid (ZA, Z-5744 LKT laboratories, St. Paul, MN) two times per week, for 1 week prior to periapical disease and CIA induction. The rationale for this 1-week pre-treatment was to induce bone turnover suppression at the time of dental intervention. Vehicle or ZA treatment continued for 8 additional weeks for a total duration of nine weeks for the experiment. Also, at week 4 of the experiment, and three weeks after the original injection to induce CIA, a booster injection of type-II collagen in IFA was performed (see bellow). ZA dose was used to increase the incidence of ONJ-like lesions in mice, as described previously.[30] The protocol followed all

recommendations of the ARRIVE (Animal Research: Reporting in Vivo Experiments) guidelines for execution and submission of studies in animals.[34]

Induction of periapical disease

We have established an ONJ mouse model employing experimental periapical disease.[30,33] To induce periapical disease, the pulp chamber of the right 1st and 2nd mandibular molars were accessed utilizing a stainless-steel ¼ size round bur in a high speed handpiece, avoiding furcal perforation, and the root canals were left exposed to the oral environment for lesion induction. The crowns of the left 1st and 2nd molars were kept intact.

Spontaneous naturally occurring peri-radicular disease

Naturally and spontaneously occurring peri-radicular disease have been reported in mice.[35–37] We have observed ONJ like lesions around such lesions in mice treated with high doses of antiresorptives [31] Such diseased maxillary sites, identified by periradicular osteolysis and/or periosteal bone formation by μCT imaging, were compared to sites with healthy dento-alveolar structures, as previously described.[31]

Induction of collagen-induced arthritis (CIA)

CIA was established following precisely previous published protocol.[38] Briefly, bovine type-II collagen (Chondrex 20021; BD Biosciences, San Jose, CA, USA) was dissolved at 4 mg/mL in 0.1 M acetic acid at 4°C. Complete Freund's adjuvant (CFA) was composed of incomplete Freund's adjuvant (IFA) (Sigma Aldrich – F5506) and freshly ground heat-killed *Mycobacterium tuberculosis* strain H37Ra (BD Biosciences, San Jose, CA, USA). A 1:1 (v/v) emulsion consisting of collagen (100 μg) and CFA (100 μg of *M. tuberculosis*) was prepared. DBA1/J male mice were immunized via intradermal injection with 50 μL of the emulsion about 1.5 cm distal from the base of the tail, being careful to choose a tissue site and not a vessel. Three weeks after the primary immunization, a booster injection with 100 μg bovine type-II collagen in IFA was given in the tail at a site proximal to the first injection, about 1 cm distal from the tail base.

Clinical assessment of RA

Mice were scored for arthritis every other day from day 21 after the first immunization until the time of sacrifice using the following criteria: 0 = no joint swelling, 1 = swelling of one finger joint, 2 = mild swelling of the wrist or ankle, or 3 = severe swelling of the wrist or ankle, as described.[39] The scores for all fingers of forepaws and hind paws, wrists and ankles were totaled for each mouse (with a maximum possible score of 12 for each mouse).

Animal sacrifice and analyses

After 9 weeks of treatment, six animals from the control and experimental groups were sacrificed via isoflurane overdose. The mandibles, maxillae, tibias, femurs and hind paws were carefully harvested, and the block samples were fixed in 4% paraformaldehyde for 48 hours and stored in 70% ethanol at room temperature until they were scanned using a μCT system.

Micro-computed tomography scanning (μCT scanning)

Maxillae, mandibles, femurs, tibiae and hind paws were scanned using a μCT imaging system (μCT Skyscan 1172; Skyscan, Kontich, Belgium) as described.[30–33] For linear measurements, volumetric image data were converted to Digital Imaging and Communications in Medicine (DICOM) format and imported in the Dolphin Imaging software (Chatsworth, CA) to generate 3D and multiplanar reconstructed images.

In the mandible, periapical bone loss (the distance from the root apex to the periapical alveolar bone) was measured at the distal root of the first and the mesial root of the second molars in a sagittal slice. The lamina dura thickness and the width of the periodontal ligament (PDL) space were quantified through the middle of the furcation area of the first molar along the mesial-distal axis of the tooth, in a sagittal slice. The lingual and buccal bone thickness was measured in an axial slice at the level of the apical third or the root for the first and second molar comprising the shortest distance from the lingual surface of the root to the outline of the alveolar ridge. In the maxilla, the cement-enamel junction (CEJ) to the alveolar bone crest (ABC) distance was measured at the distal surface of the first molar. The lamina dura thickness, width of the PDL space and lingual bone thickness were measure in the same manner as in the mandible. All measurements were performed according to previous studies.[30–33]

Alveolar bone volume (BV), tissue volume (TV) and BV/TV analysis were assessed using the CTAn software (Skyscan, Kontich, Belgium). A region of interest (ROI) was delimitated from the root apices to the alveolar crest, and from the mesial root of the first molar to the distal root of the third molar. Teeth roots and periodontal ligament were excluded from the ROI.

Analysis in the femurs and tibiae was performed using CTAn on transaxial datasets for the proximal epiphyseal bone. ROIs of distal femur metaphysis and proximal tibia metaphysis included the trabecular but excluded the cortical bone. Greyscale thresholds for quantitation of structural parameters were determined using the thresholding algorithm within CTAn software. BV, TV, BV/TV, trabecular number (Tb.N), trabecular thickness (Tb.Th), and trabecular separation (Tb.Sp) were determined.

Histologic analyses

Mandible, maxilla, femur, tibia and hind paws were decalcified in 14.5% EDTA. Samples were paraffin embedded, 4 μm thick serial sections were obtained and stained with hematoxylin and eosin (H&E). All H&E stained slides were digitally scanned at 20x magnification using the Aperio AT automated slide scanner. An operator blinded to the specimen identity performed the histological measurements. Using the ruler tool in Aperio ImageScope software (Aperio Technologies, Inc., Vista, CA, USA), 1-mm of the alveolar bone starting from the alveolar crest was identified. This height extended to near the floor of the maxillary sinus in the maxilla and the mandibular canal in the mandible. For the maxilla, the region of interest (ROI) from the buccal cortex to the mid-palatal suture, while from the mandible, the ROI extended from the buccal to the lingual cortices.

Epithelium to alveolar crest distance was measured in the palatal side of the maxilla and in the lingual side of the mandible. To quantify periosteal bone thickness, the ruler tool was used to measure the three greatest areas of the buccal periosteal thickness that were then averaged. All the measurements were performed according to published studies.[30,31,33]

Within the ROI, the total number of empty osteocytic lacunae and the osteonecrotic area(s), defined as a loss of more than five contiguous osteocytes were measured. Lacunae housing necrotic, karyolitic osteocytes, indicated by eosinophilic stained nuclei, were counted as empty osteocytes. Lacunae, both empty and containing osteocytes, were counted manually and the ratio of empty to total lacunae in the ROI was calculated. The Aperio ImageScope software (Aperio, Vista, CA, USA) has an automated tool, the surface area tool, which was used to measure the area of osteonecrosis and the total bone area. The % osteonecrotic area was determined by dividing the surface area of osteonecrosis, as calculated by the software, by the total bone area, as calculated by the software, and multiplying by 100.

For standard histologic assessment in the knees and paws, sagittal sections (4 μm) were stained with H&E to study synovial inflammation, and to determine cartilage and bone destruction. Histopathologic changes were scored as described.[40–42] Briefly, infiltration of cells was scored in a scale of 0–3, depending on the amount of inflammatory cells in the synovial cavity and synovial tissues (0 = no cells, 1 = mild cellularity, 2 = moderate cellularity, and 3 = maximal cellularity). Cartilage destruction was distinctly graded on a scale of 0–3, ranging from the non-appearance of dead chondrocytes (empty lacunae) to a complete loss of chondrocytes in the cartilage. Bone erosion was scored on a scale of 0 to 5 ranging from no damage to complete bone loss.[40] Histopathologic changes in the knee joints were scored in the femur/tibia region. For the ankle joint, we scored the calcaneus and ankle region. Scoring was done in a blinded manner.

To assess osteoclast numbers, sections were stained using the Leukocyte Acid Phosphatase 387-A kit (Sigma-Aldrich, St. Louis, MO, USA). TRAP-positive multinucleated cells containing 2 or more nuclei were counted in the mandible, maxilla, ankle and knee in a total of 6 mice per group.

Histology and digital imaging was done at the UCLA Translational Pathology Core Laboratory.

Statistics

Analyses were performed on GraphPad Prism Software (GraphPad Software, Inc., La Jolla, CA). Group measures were expressed as mean and the standard error of the mean (SEM). Statistical significance was assessed using two-way analysis of variance (ANOVA) followed by the Bonferroni post-hoc test for multiple comparisons among groups. Data between groups (healthy vs. diseased) were compared using the Student's t test. Dental disease, osteonecrosis and bone exposure were also recorded as present or absent. These categorical data (Table 1) were analyzed using the Fisher's exact test.

RESULTS

Radiographic features of ONJ in the maxilla and mandible

μCT of healthy maxillae in all groups showed normal alveolar crest extending just inferior of the CEJ, around the molar roots with absence of bone expansion and bone loss (Figure 1, A–D). On the other hand, diseased vehicle and CIA mice demonstrated substantial bone destruction and loss of crest height increasing the distance between the CEJ to the alveolar bone, extending almost to the root apex of the 1st molar. Substantial palatal and buccal bone expansion of the alveolar ridge were also observed (Figure 1, A1 and C1). Bone loss was also present for the ZA and CIA-ZA mice, however the extent of bone loss was significantly reduced and was associated with extensive areas of new periosteal bone apposition, which resulted in substantial expansion of the palatal and buccal thickness of the maxillary alveolar ridge (Figure 1, B1 and D1). Similar findings were observed for the mandible in non-drilled and drilled sites of all groups (Supplemental Figure 1).

To quantitate bone loss, the CEJ to ABC distance were measured. In the healthy side of all animals a short CEJ to ABC distance was observed (Figure 2, A–D and E). Significantly increased distance was observed for vehicle and CIA mice with dental disease, indicating significant bone loss (Figure 2, A1, C1 and E; white arrows). As expected, in ZA and CIA-ZA mice this distance was reduced, although CIA-ZA animals showed significantly more bone loss compared to ZA treated mice (Figure 2, B1, D1 and E). Similar findings were seen in the mandibles with periapical disease (Supplemental Figure 2, A–D1 and E).

We then quantified the changes in the lamina dura thickness and PDL space width in sagittal slices, at the furcation area of the 1st molar. In the healthy side of all animals, a uniform lamina dura thickness and PDL space were observed albeit in mice with antiresorptive treatment, increased lamina dura thickness was noted (Figure 2, A–D and F–G). In the diseased site of vehicle and CIA mice, there was significant loss of lamina dura thickness and significant increase of PDL space width (Figure 2, A1, C1, F and G). ZA and CIA-ZA treated mice demonstrated increased lamina dura thickness and PDL space preserved. Statistically significant inhibition of PDL widening was observed for ZA treated mice compared to other groups (Figure 2, B1, D1, F and G). Comparable results were also noted in mandibular teeth (Supplemental Figure 2, A–D1, F and G).

Then, the palatal and buccal bone thickness at the apical third of the molar roots was measured on axial slices. Healthy site of all mice showed normal palatal and buccal bone thickness without bone expansion (Figure 2, H and I–L). As previously reported,[31,32] significant expansion of the alveolar bone with exuberant osteolysis was noted for dental diseased vehicle and CIA treated mice (Figure 2, H and I1, K1). In contrast, ZA and CIA-ZA treated mice exhibited increased bone thickness (Figure 2, H and J1, L1). Importantly, in CIA-ZA treated mice a statistically significant difference in bone thickness was noted compared to all other groups (Figure 2, H, I1–L1; white arrowheads). Similar features were observed at the mandibular alveolar ridge (Supplemental Figure 2, H–K1, L; yellow arrows).

To assess the overall effects in bone structure, BV, TV and BV/TV of the alveolar bone were measured. Dental disease in vehicle and CIA mice decreased BV, and BV/TV, while

antiresorptive treatment substantially increased all of these measurements compared to the vehicle and CIA mice (Supplemental Figure 3, A, A1, D, D1 and E–G; white arrows). Interestingly, CIA-ZA mice showed slightly higher BV compared to the ZA animals probably due to increased periosteal bone deposition in the buccal side (Supplemental Figure 3, D1; arrowheads and Supplemental Figure 4).

Increased severity of ONJ in CIA mice treated with ZA

To evaluate histologic features of ONJ, coronal sections were obtained between the 1st and 2nd molars. All healthy groups showed normal alveolar bone (Figure 3, A, C, E, G; turquoise arrow), marginal epithelium (Figure 3, A, C, E, G; red arrows), PDL and absence of inflammatory infiltrate. In diseased vehicle and CIA mice, abundant inflammatory infiltrate (Figure 3, B–B1, F–F1), periosteal bone deposition and bone resorption were noted (Figure 3, B–B1). The reduction of the alveolar crest height in the diseased site of vehicle and CIA treated mice resulted in an increase of the distance between the marginal epithelium to the ABC (Figure 3, B–B1, F–F1; turquoise and red arrows). No histologic evidence of osteonecrosis was observed in any of the samples.

Infiltrate of inflammatory cells was also noted in the diseased site of ZA and CIA-ZA mice appearing more intense in the CIA-ZA mice (Figure 3, D, D1, H, H1; Supplemental Figure 5). Reduced alveolar bone loss resulted in reduction of the epithelial to the ABC distance (Figure 3, D, H; turquoise and red arrows; Supplemental Figure 5). Empty osteocytic lacunae, areas of osteonecrosis (Figure 3, D–D1, H–H1; yellow arrows; Supplemental Figure 5) and periosteal new bone formation (Figure 3, D–D1, H–H1; Supplemental Figure 5) were observed for both ZA and CIA-ZA treated mice. Interestingly, necrotic bone was not covered by epithelium and was exposed to the oral environment in 7 mice for CIA-ZA treated mice compared with 3 mice for ZA treated mice (Figure 3, D, –D1, H–H1; green arrows, Table 1). Importantly, areas of osteonecrosis were significantly more extensive in CIA-ZA compared to ZA treated animals (Figure 3, D–D1, H–H1; yellow arrows; Supplemental Figure 5). Similar observations were seen in healthy and drilled sites of the mandible (Supplemental Figure 5).

Quantification of histologic findings demonstrated a statistically significant increase in the distance between the marginal epithelium to the ABC in diseased sites of vehicle and CIA mice. This distance was decreased in ZA and CIA-ZA mice (Figure 3, I). Importantly, the marginal epithelium to the ABC distance was significantly smaller in the CIA-ZA mice compared to all other groups. Number of empty osteocytic lacunae and area of osteonecrosis were measured at the area of the alveolar ridge for healthy and diseased treatment groups. No areas of osteonecrosis were seen in the healthy or diseased sites of the vehicle and CIA treated mice. Presence of empty osteocytic lacunae was not statistically significant between vehicle and CIA treated mice (Figure 3, J and K). Significant increase in empty osteocytic lacunae and areas of osteonecrosis were observed in diseased sites of ZA and CIA-ZA treated mice (Figure 3, J and K). Importantly, statistically significant increase in areas of osteonecrosis and empty osteocytic lacunae were present in CIA-ZA compared to ZA treated animals (Figure 3, J and K; Supplemental Figure 5). Osteonecrotic areas in ZA treated mice without or with CIA extended in significant part of the alveolar ridge and close to the buccal

or lingual mandibular cortex in the mandible or the buccal and palatal cortex or the maxillary sinus floor in the maxilla (Supplemental Figure 6).

Few TRAP + cells were noted at the healthy site of all treatment groups. In contrast, diseased sites of all groups showed statistically increase number of TRAP+ cells. TRAP+ cells in controls and CIA animals showed close attachment to the bone with extended bone contact surface. However, in ZA and CIA-ZA mice osteoclasts presented round morphology, with pyknotic nuclei, and occasionally were separated from the bone surface (Figure 4, A–H1 and I). Similar results were found for the healthy and drilled sites of the mandible (Supplemental Figure 7, A–I).

Table 1 summarizes radiographic and histologic features in maxillae and mandibles. Disease incidence such as peri-radicular and periapical disease ranged from 50–62.5% without statistical differences among groups. Areas of osteonecrosis and bone exposure were present only in the ZA and CIA-ZA treated mice. Osteonecrotic areas ranged, in the diseased sites of ZA and CIA-ZA, from 64.3–86.7%, respectively. Interestingly, in CIA-ZA group bone exposure was 2.3-fold higher than ZA treated animals ranging from 21.4–46.7% of the diseased mice.

Changes in clinical course and severity of rheumatoid arthritis

The clinical course of arthritis in DBA-1J mice injected with collagen is shown in Figure 5, A–D3. The rate of clinical CIA progression after onset was not statistically significant altered by ZA treatment. ZA-treated CIA mice showed a slightly reduced severity of clinical arthritis, which was not significant compared to the CIA group (Figure 5, E). Paw thickness and paw swelling were also not significant between veh vs. ZA groups.

To further elucidate bone changes in the hind paws and knee joints, μCT assessment was performed. CIA treated mice demonstrated loss of bone integrity and extensive areas of erosions in the interphalangeal, ankle and calcaneus regions as well as in the knee joints with areas of periosteal new bone formation. Treatment with ZA completely abolished bone erosions but not periosteal formation (data not shown).

Histological analysis of the hind paws and knee joints (Figure 6, A–D1 and E–F) revealed absence of synovitis or inflammatory bone changes in vehicle and ZA treated mice (Figure 6, A–B1 and E). In contrast, CIA and CIA-ZA treated mice showed inflammatory infiltrate in the ankle, calcaneus and knee (Figure 6, C–D1 and E; black arrows). CIA treated mice presented with cartilage and bone resorption (Figure 6, C–C1, F), while ZA treatment protected and maintained cartilage and bone architecture of the ankle, calcaneus and knee joints (Figure 6, D–D1, F). No osteonecrosis was seen adjacent to the inflammatory areas in CIA or CIA-ZA groups.

Finally, to investigate the overall effects of ZA in osteoclast numbers TRAP staining was performed. As expected, significant increase in TRAP + cells were noted for the CIA treated mice. ZA treated CIA mice showed increased number of positive TRAP cells compared to the vehicle and ZA treated mice, but this difference was not significant (Figure 6, G).

DISCUSSION

Clinical studies suggest an increased incidence of ONJ in patients with RA.[8,20,28,29,43] The potential link between RA and ONJ could be due to common etiologic factors of the two diseases.[43] Indeed, RA is a chronic systemic immunologic disease that features persistent high level of proinflammatory cytokines and inflammatory cells very much like other inflammatory diseases in the mouth such as periodontitis and periapical disease.[41] Periodontal and periapical disease are infectious processes mediated and modulated by the host immune system[44–47] and have been considered ONJ risk factors.[20] Furthermore, an increased inflammatory response that might implicate a role of gamma-delta T-cells, release of pro-inflammatory cytokines, increased oxidative stress, and intensified tissue destruction are common denominators in both RA and ONJ.[15,43] Additionally, increased bacterial infection in RA patients could increase the risk and complicate the course of ONJ.[15,43]

Biologic agents, DMARDs and immunosuppressive agents such as methotrexate, NSAIDs, steroids and bisphosphonates have led to substantial long-term improvements in patients with RA.[48–50] However, biologics agents increase the risk of opportunistic infections,[51] corticosteroids have been shown to impair bone and wound healing,[52] methotrexate may affect bone healing through inhibition of osteoblastic proliferation and bone turnover suppression,[53] steroids reduce bone remodeling,[54] suppress bone turnover and angiogenesis, result in osteoblast and osteocyte apoptosis,[55] increasing the risk for infection and necrosis.[56] Furthermore, these common medications for RA including steroids and methotrexate have been associated with ONJ.[8,15,27,57,58]

Whether RA itself or medications used for RA management potentially exacerbate ONJ occurrence and severity is not known.[8,43] Given the low incidence of ONJ, particularly in patients treated with low dose BPs, clinical studies can be limited in providing accurate causal association between the two diseases, particularly in the presence of confounding variables.[18,21] Animal studies can complement clinical findings, since they can be designed in a controlled environment, where experimental variables are more predictable and adjustable. Several animal models of ONJ have been reported that provide powerful tools in assessing disease pathophysiology.[30–33,59,60] In the studies presented herein, we employed two mouse ONJ models in animals treated with high levels ZA in the absence of tooth extractions, but in the presence of either experimental periapical disease or naturally occurring periradicular infection.[30–32] We have reported that these animals develop ONJ-like lesions with clinical bone exposure, and radiographic and histologic features, such as periosteal bone formation, bone sclerosis, thickening of lamina dura, empty presence of osteocytic lacunae, and osteonecrosis resembling the human disease.[30–33,59]

We also utilized the well-established CIA mouse model to induce aggressive arthritis with RA features such as paw swelling, synovial inflammation and focal erosions at the joints.[61] Similar to our previous observations,[30–33] dental disease resulted in periradicular inflammation and bone loss reflected by increased CEJ to ABC distance and PDL space width, decreased BV, BV/TV, lamina dura and lingual bone thickness, increased inflammatory infiltrate and marginal epithelium to the ABC distance. No statistical

differences in quantitative indices of alveolar bone loss between control and CIA mice were noted, suggesting that CIA did not complicate periapical or periradicular disease.

Radiographic assessment demonstrated that ZA treatment prevented bone changes and increased the overall alveolar bone volume in the diseased sites even in the presence of CIA. Interestingly, CIA-ZA group demonstrated increased bone thickness for both palatal/lingual and buccal sides probably due to increased periosteal bone formation compared to all the other groups. Histologically, successful induction of ONJ-like lesions was observed in both ZA and CIA-ZA treated mice, including presence of empty osteocytic lacunae and areas of osteonecrosis. Importantly, in ZA treated CIA mice significant differences in empty osteocytic lacunae number and osteonecrotic area, as well as in areas of exposed bone were observed, characterizing a more severe incidence and development of ONJ. Notably, in these experiments, mice were not treated with agents utilized for the management of RA, and any increased burden of ONJ in CIA-ZA mice should be attributed to the effects of heightened systemic effects induced by collagen injection in these animals. In our experiments, although the number of animals with osteonecrosis in the CIA-ZA group was higher than that in the ZA group, the results did not reach statistical significance. This was most probably due to the number of animals. Collectively, our findings suggest that RA complicates ONJ severity and possibly incidence in the mouse models employed, and suggest that RA might be a risk factor for ONJ.

Clinical features of RA, including paw swelling, redness, and sometimes ankylosis of the hind paws were observed in both CIA and CIA-ZA treated mice. As expected, [50,61–63] cartilage destruction, bone erosions and periosteal bone formation in animals with CIA was present. Similar to previously published data,[50] inhibition of bone destruction, but presence of periosteal bone formation was seen in CIA-ZA mice. These results parallel observations with the osteoclastogenesis inhibitor osteoprotegerin (OPG), emphasizing the preeminence of osteoclastic activity in mediating bone destruction.[61,63]

Although, extensive osteonecrosis was seen in the maxilla and mandible around areas of periapical or periradicular inflammation, no areas of osteonecrosis were observed in the interphalangeal and knee joints in CIA-ZA mice, despite the robust synovial and periarticular inflammation. This disparate response of the jaws vs. other bones to inflammation could be due to basic differences in the inflammatory conditions around the jaws vs. long bone joints. Both periapical or periradicular inflammation are caused by bacterial infection[18,64] while the collagen-induced periarticular inflammation develops in sterile conditions. Alternatively, the presence of osteonecrosis in the maxilla and mandible could be due to a unique response of the jaws vs. other bones to the harmful inflammatory environment. Such a heightened sensitivity could explain the near exclusive presentation of ONJ in the jaws compared to the remaining skeleton.[18,64]

As our data are translated in the clinical setting, three considerations should be made. First, the ZA doses administered to the animals parallel those for oncologic patients.[65,66] We utilized these higher doses to increase the incidence of ONJ in mice without or with CIA, such that we could derive statistically significant conclusions. Given the fact that most RA patients receive much lower BP doses for the management of osteoporosis,[1,8,28] the ONJ

incidence in these patients is expected to be lower that observed in the CIA-ZA animals. Nevertheless, despite the anticipated lower disease incidence with lower BP doses, our data suggest a relative increase in ONJ burden in patients with RA.

A second consideration is that our models utilized dental disease as the initiating factor for ONJ. Although dental disease is associated with ONJ occurrence[20] and is considered a local risk factor for the disease[18,21], the major local precipitating factor associated with ONJ is dentoalveolar surgery and particularly tooth extraction.[67–69] We elected not to utilize tooth extraction in our models, as we intended to explore the impact of RA in the early phases of ONJ development prior to surgical intervention.

A final consideration is that our studies did not address the potential effect of RA treatment modalities as risk factors for ONJ. It would be expected that such pharmacologic agents would have a detrimental effect in the response of the alveolar bone to osteonecrosis development. However, these treatments would reduce the systemic inflammatory response of CIA and would attenuate its negative consequences in ONJ development. Clearly, further studies utilizing appropriate animal models are required to assess the association of specific RA treatment regimens and ONJ pathogenesis.

In summary, using two different ONJ mouse models, we report at radiographic and histologic level, that ZA treated CIA mice caused more extensive ONJ changes in the maxilla and mandible. Osteonecrosis in long bones or in the ankle was not observed even in the presence of abundant inflammatory cells infiltration in the synovium. Moreover, ZA treatment completely abolished cartilage and bone destruction but not synovitis. Accordingly, high-dose administration of BPs, combined with dental disease and RA, might increase the risk for ONJ development and severity. Indeed, to the best of our knowledge, this is the first animal study to show that RA might be a risk factor for ONJ.

Supplementary Material

Refer to Web version on PubMed Central for supplementary material.

Acknowledgments

This work was supported by NIH/NIDCR R01 DE019465 (ST) and R21 DE023901 (FQP). de Molon RS was supported by the State of Sao Paulo Research Foundation (FAPESP) #2012/09968-5, the Coordination for the Improvement of Higher Level -or Educational- Personnel (CAPES) #11575/31-1 and the Lemann Foundation.

References

1. Scott DL, Wolfe F, Huizinga TW. Rheumatoid arthritis. Lancet. 2010; 376:1094–108. [PubMed: 20870100]
2. Firestein GS. Evolving concepts of rheumatoid arthritis. Nature. 2003; 423:356–61. [PubMed: 12748655]
3. Gravallese EM, Harada Y, Wang JT, Gorn AH, Thornhill TS, Goldring SR. Identification of cell types responsible for bone resorption in rheumatoid arthritis and juvenile rheumatoid arthritis. Am J Pathol. 1998; 152:943–51. [PubMed: 9546355]
4. Gough A, Sambrook P, Devlin J, et al. Osteoclastic activation is the principal mechanism leading to secondary osteoporosis in rheumatoid arthritis. J Rheumatol. 1998; 25:1282–9. [PubMed: 9676757]

5. Tanaka Y. Recent progress and perspective in JAK inhibitors for rheumatoid arthritis: from bench to bedside. J Biochem. 2015
6. Russell G, Mueller G, Shipman C, Croucher P. Clinical disorders of bone resorption. Novartis Found Symp. 2001; 232:251–67. discussion 67–71. [PubMed: 11277085]
7. Clayton ES, Hochberg MC. Osteoporosis and osteoarthritis, rheumatoid arthritis and spondylarthropathies. Curr Osteoporos Rep. 2013; 11:257–62. [PubMed: 24085651]
8. Lescaille G, Coudert AE, Baaroun V, et al. Osteonecrosis of the jaw and nonmalignant disease: is there an association with rheumatoid arthritis? J Rheumatol. 2013; 40:781–6. [PubMed: 23504384]
9. Lee SG, Park YE, Park SH, et al. Increased frequency of osteoporosis and BMD below the expected range for age among South Korean women with rheumatoid arthritis. Int J Rheum Dis. 2012; 15:289–96. [PubMed: 22709491]
10. Bock O, Felsenberg D. Bisphosphonates in the management of postmenopausal osteoporosis--optimizing efficacy in clinical practice. Clin Interv Aging. 2008; 3:279–97. [PubMed: 18686751]
11. Berenson JR, Lipton A. Bisphosphonates in the treatment of malignant bone disease. Annu Rev Med. 1999; 50:237–48. [PubMed: 10073275]
12. Black DM, Delmas PD, Eastell R, et al. Once-yearly zoledronic acid for treatment of postmenopausal osteoporosis. N Engl J Med. 2007; 356:1809–22. [PubMed: 17476007]
13. Boonen S, Laan RF, Barton IP, Watts NB. Effect of osteoporosis treatments on risk of non-vertebral fractures: review and meta-analysis of intention-to-treat studies. Osteoporos Int. 2005; 16:1291–8. [PubMed: 15986101]
14. Cranney A, Wells G, Willan A, et al. Meta-analyses of therapies for postmenopausal osteoporosis. II. Meta-analysis of alendronate for the treatment of postmenopausal women. Endocr Rev. 2002; 23:508–16. [PubMed: 12202465]
15. Conte-Neto N, Bastos AS, Marcantonio RA, Junior EM. Epidemiological aspects of rheumatoid arthritis patients affected by oral bisphosphonate-related osteonecrosis of the jaws. Head Face Med. 2012; 8:5. [PubMed: 22376948]
16. Adler RA, Fuleihan GE, Bauer DC, et al. Managing Osteoporosis in Patients on Long-Term Bisphosphonate Treatment: Report of a Task Force of the American Society for Bone and Mineral Research. J Bone Miner Res. 2015
17. Ruggiero SL, Mehrotra B, Rosenberg TJ, Engroff SL. Osteonecrosis of the jaws associated with the use of bisphosphonates: a review of 63 cases. J Oral Maxillofac Surg. 2004; 62:527–34. [PubMed: 15122554]
18. Khan AA, Morrison A, Hanley DA, et al. Diagnosis and management of osteonecrosis of the jaw: a systematic review and international consensus. J Bone Miner Res. 2015; 30:3–23. [PubMed: 25414052]
19. Khosla S, Burr D, Cauley J, et al. Bisphosphonate-associated osteonecrosis of the jaw: report of a task force of the American Society for Bone and Mineral Research. J Bone Miner Res. 2007; 22:1479–91. [PubMed: 17663640]
20. Marx RE, Sawatari Y, Fortin M, Broumand V. Bisphosphonate-induced exposed bone (osteonecrosis/osteopetrosis) of the jaws: risk factors, recognition, prevention, and treatment. J Oral Maxillofac Surg. 2005; 63:1567–75. [PubMed: 16243172]
21. Ruggiero SL, Dodson TB, Fantasia J, et al. American Association of Oral and Maxillofacial Surgeons position paper on medication-related osteonecrosis of the jaw--2014 update. J Oral Maxillofac Surg. 2014; 72:1938–56. [PubMed: 25234529]
22. Aghaloo T, Hazboun R, Tetradis S. Pathophysiology of Osteonecrosis of the Jaws. Oral Maxillofac Surg Clin North Am. 2015; 27:489–96. [PubMed: 26412796]
23. Allen MR, Burr DB. The pathogenesis of bisphosphonate-related osteonecrosis of the jaw: so many hypotheses, so few data. J Oral Maxillofac Surg. 2009; 67:61–70. [PubMed: 19371816]
24. Allen MR, Ruggiero SL. A review of pharmaceutical agents and oral bone health: how osteonecrosis of the jaw has affected the field. Int J Oral Maxillofac Implants. 2014; 29:e45–57. [PubMed: 24451887]
25. Khan A, Morrison A, Cheung A, Hashem W, Compston J. Osteonecrosis of the jaw (ONJ): diagnosis and management in 2015. Osteoporos Int. 2015

26. Zhang Q, Yu W, Lee S, Xu Q, Naji A, Le AD. Bisphosphonate Induces Osteonecrosis of the Jaw in Diabetic Mice via NLRP3/Caspase-1-Dependent IL-1beta Mechanism. J Bone Miner Res. 2015
27. Conte-Neto N, Bastos AS, Spolidorio LC, Marcantonio RA, Marcantonio E Jr. Oral bisphosphonate-related osteonecrosis of the jaws in rheumatoid arthritis patients: a critical discussion and two case reports. Head Face Med. 2011; 7:7. [PubMed: 21524309]
28. Landesberg R, Taxel P. Osteonecrosis of the jaw and rheumatoid arthritis. Is it the disease or the drugs? J Rheumatol. 2013; 40:749–51. [PubMed: 23728184]
29. Park W, Kim NK, Kim MY, Rhee YM, Kim HJ. Osteonecrosis of the jaw induced by oral administration of bisphosphonates in Asian population: five cases. Osteoporos Int. 2010; 21:527–33. [PubMed: 19484166]
30. Aghaloo TL, Cheong S, Bezouglaia O, et al. RANKL inhibitors induce osteonecrosis of the jaw in mice with periapical disease. J Bone Miner Res. 2014; 29:843–54. [PubMed: 24115073]
31. de Molon RS, Cheong S, Bezouglaia O, et al. Spontaneous osteonecrosis of the jaws in the maxilla of mice on antiresorptive treatment: a novel ONJ mouse model. Bone. 2014; 68:11–9. [PubMed: 25093262]
32. de Molon RS, Shimamoto H, Bezouglaia O, et al. OPG-Fc but Not Zoledronic Acid Discontinuation Reverses Osteonecrosis of the Jaws (ONJ) in Mice. J Bone Miner Res. 2015; 30:1627–40. [PubMed: 25727550]
33. Kang B, Cheong S, Chaichanasakul T, et al. Periapical disease and bisphosphonates induce osteonecrosis of the jaws in mice. J Bone Miner Res. 2013; 28:1631–40. [PubMed: 23426919]
34. Kilkenny C, Browne WJ, Cuthill IC, Emerson M, Altman DG. Improving bioscience research reporting: the ARRIVE guidelines for reporting animal research. Osteoarthritis Cartilage. 2012; 20:256–60. [PubMed: 22424462]
35. Clarke MC, Taylor RJ, Hall GA, Jones PW. The occurrence in mice of facial and mandibular abscesses associated with Staphylococcus aureus. Lab Anim. 1978; 12:121–3. [PubMed: 152826]
36. Grant N, Jackson K, Lee R, Scharf B. Mandibular mass in a young Swiss-Webster mouse. Lab Anim (NY). 2002; 31:25–6. [PubMed: 12200582]
37. Lawson GW. Etiopathogenesis of mandibulofacial and maxillofacial abscesses in mice. Comp Med. 2010; 60:200–4. [PubMed: 20579435]
38. Brand DD, Latham KA, Rosloniec EF. Collagen-induced arthritis. Nat Protoc. 2007; 2:1269–75. [PubMed: 17546023]
39. Komatsu N, Okamoto K, Sawa S, et al. Pathogenic conversion of Foxp3+ T cells into TH17 cells in autoimmune arthritis. Nat Med. 2014; 20:62–8. [PubMed: 24362934]
40. Coppieters K, Dreier T, Silence K, et al. Formatted anti-tumor necrosis factor alpha VHH proteins derived from camelids show superior potency and targeting to inflamed joints in a murine model of collagen-induced arthritis. Arthritis Rheum. 2006; 54:1856–66. [PubMed: 16736523]
41. de Aquino SG, Abdollahi-Roodsaz S, Koenders MI, et al. Periodontal pathogens directly promote autoimmune experimental arthritis by inducing a TLR2- and IL-1-driven Th17 response. J Immunol. 2014; 192:4103–11. [PubMed: 24683190]
42. Marijnissen RJ, Roeleveld DM, Young D, et al. Interleukin-21 receptor deficiency increases the initial toll-like receptor 2 response but protects against joint pathology by reducing Th1 and Th17 cells during streptococcal cell wall arthritis. Arthritis Rheumatol. 2014; 66:886–95. [PubMed: 24757141]
43. Conte Neto N, Bastos AS, Chierici-Marcantonio RA, Marcantonio E Jr. Is rheumatoid arthritis a risk factor for oral bisphosphonate-induced osteonecrosis of the jaws? Med Hypotheses. 2011; 77:905–11. [PubMed: 21885199]
44. de Molon RS, de Avila ED, Cirelli JA. Host responses induced by different animal models of periodontal disease: a literature review. J Investig Clin Dent. 2013; 4:211–8.
45. de Molon RS, de Avila ED, Boas Nogueira AV, et al. Evaluation of the host response in various models of induced periodontal disease in mice. J Periodontol. 2014; 85:465–77. [PubMed: 23805811]
46. de Molon RS, Mascarenhas VI, de Avila ED, et al. Long-term evaluation of oral gavage with periodontopathogens or ligature induction of experimental periodontal disease in mice. Clin Oral Investig. 2015; epub ahead of print. doi: 10.1007/s00784-015-1607-0

47. Cavagni J, de Macedo IC, Gaio EJ, et al. Obesity and Hyperlipidemia Modulate Alveolar Bone Loss in Wistar Rats. J Periodontol. 2016; 87:e9–e17. [PubMed: 26376945]
48. Ward MM. Decreases in rates of hospitalizations for manifestations of severe rheumatoid arthritis, 1983–2001. Arthritis Rheum. 2004; 50:1122–31. [PubMed: 15077294]
49. Finckh A, Choi HK, Wolfe F. Progression of radiographic joint damage in different eras: trends towards milder disease in rheumatoid arthritis are attributable to improved treatment. Ann Rheum Dis. 2006; 65:1192–7. [PubMed: 16540549]
50. Sims NA, Green JR, Glatt M, et al. Targeting osteoclasts with zoledronic acid prevents bone destruction in collagen-induced arthritis. Arthritis Rheum. 2004; 50:2338–46. [PubMed: 15248235]
51. Giles JT, Bartlett SJ, Gelber AC, et al. Tumor necrosis factor inhibitor therapy and risk of serious postoperative orthopedic infection in rheumatoid arthritis. Arthritis Rheum. 2006; 55:333–7. [PubMed: 16583385]
52. Howe CR, Gardner GC, Kadel NJ. Perioperative medication management for the patient with rheumatoid arthritis. J Am Acad Orthop Surg. 2006; 14:544–51. [PubMed: 16959892]
53. Gerster JC, Bossy R, Dudler J. Bone non-union after osteotomy in patients treated with methotrexate. J Rheumatol. 1999; 26:2695–7. [PubMed: 10606386]
54. Patschan D, Loddenkemper K, Buttgereit F. Molecular mechanisms of glucocorticoid-induced osteoporosis. Bone. 2001; 29:498–505. [PubMed: 11728918]
55. Greenberger S, Boscolo E, Adini I, Mulliken JB, Bischoff J. Corticosteroid suppression of VEGF-A in infantile hemangioma-derived stem cells. N Engl J Med. 2010; 362:1005–13. [PubMed: 20237346]
56. Zizic TM, Marcoux C, Hungerford DS, Dansereau JV, Stevens MB. Corticosteroid therapy associated with ischemic necrosis of bone in systemic lupus erythematosus. Am J Med. 1985; 79:596–604. [PubMed: 4061472]
57. Sonis ST, Watkins BA, Lyng GD, Lerman MA, Anderson KC. Bony changes in the jaws of rats treated with zoledronic acid and dexamethasone before dental extractions mimic bisphosphonate-related osteonecrosis in cancer patients. Oral Oncol. 2009; 45:164–72. [PubMed: 18715819]
58. Christodoulou C, Pervena A, Klouvas G, et al. Combination of bisphosphonates and antiangiogenic factors induces osteonecrosis of the jaw more frequently than bisphosphonates alone. Oncology. 2009; 76:209–11. [PubMed: 19212145]
59. Aghaloo TL, Kang B, Sung EC, et al. Periodontal disease and bisphosphonates induce osteonecrosis of the jaws in the rat. J Bone Miner Res. 2011; 26:1871–82. [PubMed: 21351151]
60. Cheong S, Sun S, Kang B, et al. Bisphosphonate uptake in areas of tooth extraction or periapical disease. J Oral Maxillofac Surg. 2014; 72:2461–8. [PubMed: 25262401]
61. Romas E, Gillespie MT, Martin TJ. Involvement of receptor activator of NFkappaB ligand and tumor necrosis factor-alpha in bone destruction in rheumatoid arthritis. Bone. 2002; 30:340–6. [PubMed: 11856640]
62. Bogoch ER, Lee TC, Fornasier VL, Berger SA. Articular damage is associated with intraosseous inflammation in the subchondral bone marrow of joints affected by experimental inflammatory arthritis and is modified by zoledronate treatment. J Rheumatol. 2007; 34:1229–40. [PubMed: 17516617]
63. Redlich K, Hayer S, Maier A, et al. Tumor necrosis factor alpha-mediated joint destruction is inhibited by targeting osteoclasts with osteoprotegerin. Arthritis Rheum. 2002; 46:785–92. [PubMed: 11920416]
64. Katsarelis H, Shah NP, Dhariwal DK, Pazianas M. Infection and Medication-related Osteonecrosis of the Jaw. J Dent Res. 2015; 94:534–9. [PubMed: 25710950]
65. Ibrahim A, Scher N, Williams G, et al. Approval summary for zoledronic acid for treatment of multiple myeloma and cancer bone metastases. Clin Cancer Res. 2003; 9:2394–9. [PubMed: 12855610]
66. Maerevoet M, Martin C, Duck L. Osteonecrosis of the jaw and bisphosphonates. N Engl J Med. 2005; 353:99–102. discussion 99- [PubMed: 16003838]

67. Vahtsevanos K, Kyrgidis A, Verrou E, et al. Longitudinal cohort study of risk factors in cancer patients of bisphosphonate-related osteonecrosis of the jaw. J Clin Oncol. 2009; 27:5356–62. [PubMed: 19805682]

68. Saad F, Brown JE, Van Poznak C, et al. Incidence, risk factors, and outcomes of osteonecrosis of the jaw: integrated analysis from three blinded active-controlled phase III trials in cancer patients with bone metastases. Ann Oncol. 2012; 23:1341–7. [PubMed: 21986094]

69. Fehm T, Beck V, Banys M, et al. Bisphosphonate-induced osteonecrosis of the jaw (ONJ): Incidence and risk factors in patients with breast cancer and gynecological malignancies. Gynecol Oncol. 2009; 112:605–9. [PubMed: 19136147]

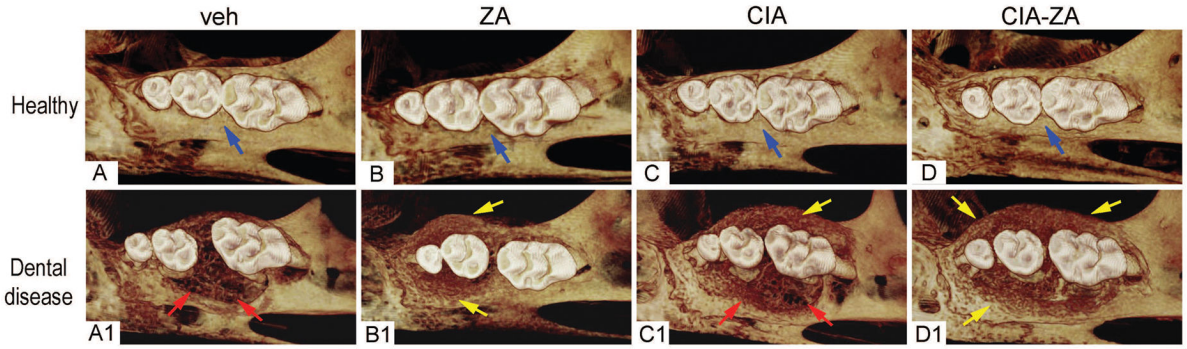

Figure 1. 3D µCT reconstructed images of maxilla

(A–D) 3D reformatted views of healthy site in vehicle, ZA, CIA and CIA-ZA, respectively. (A1–D1) 3D reformatted views of diseased site in all the groups. Blue arrows point to normal alveolar bone crest. Red arrow point to periodontal bone loss and areas of osteolysis in the diseased site of vehicle and RA treated mice. Yellow arrows point to increased bone deposition.

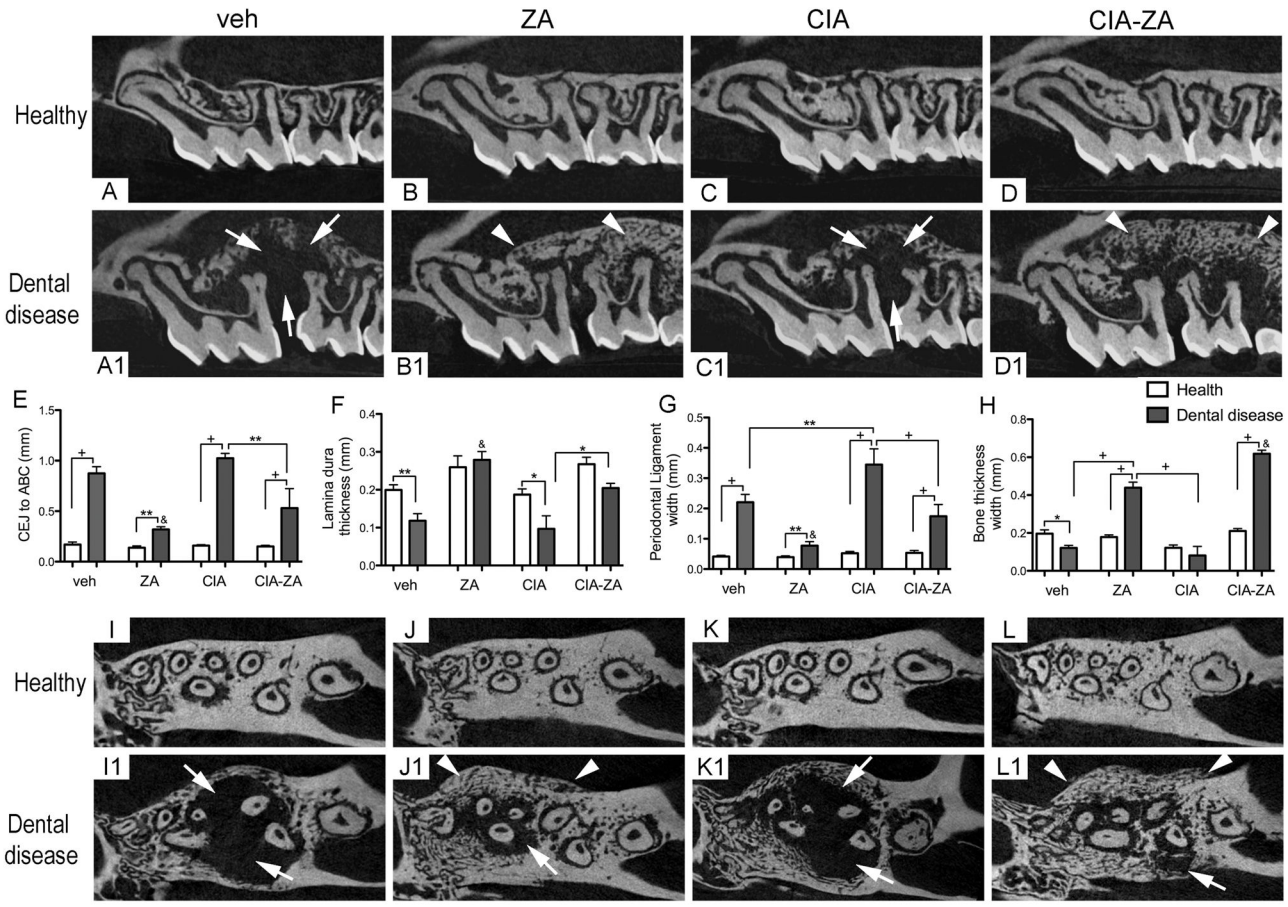

Figure 2. Sagittal and axial μCT sections through the maxillary alveolar ridge and quantification of the μCT findings

(A–D) Sagittal and (I-L) axial sections of healthy maxillae of vehicle, ZA, CIA and CIA-ZA mice, respectively. (A1–D1) Sagittal and (I1-L1) axial sections of diseased maxillae in all groups. White arrows point to areas of bone resorption and/or osteolysis. White arrowheads point to bone deposition and areas of bone expansion. (E–H) Quantification of CEJ to ABC distance, lamina dura thickness, PDL space width and palatal bone thickness in all mice, respectively. (n = 6 mice per group). & Statistically significant different compared to diseased mice, $p < 0.0001$. +Statistically significant different from indicated groups, $p < 0.0001$. **Statistically significant different from indicated groups, $p < 0.001$. *Statistically significant different from indicated groups, $p < 0.05$. Differences among groups were calculated by two-way ANOVA and between groups by Student's t test. Data represent the mean ± SEM.

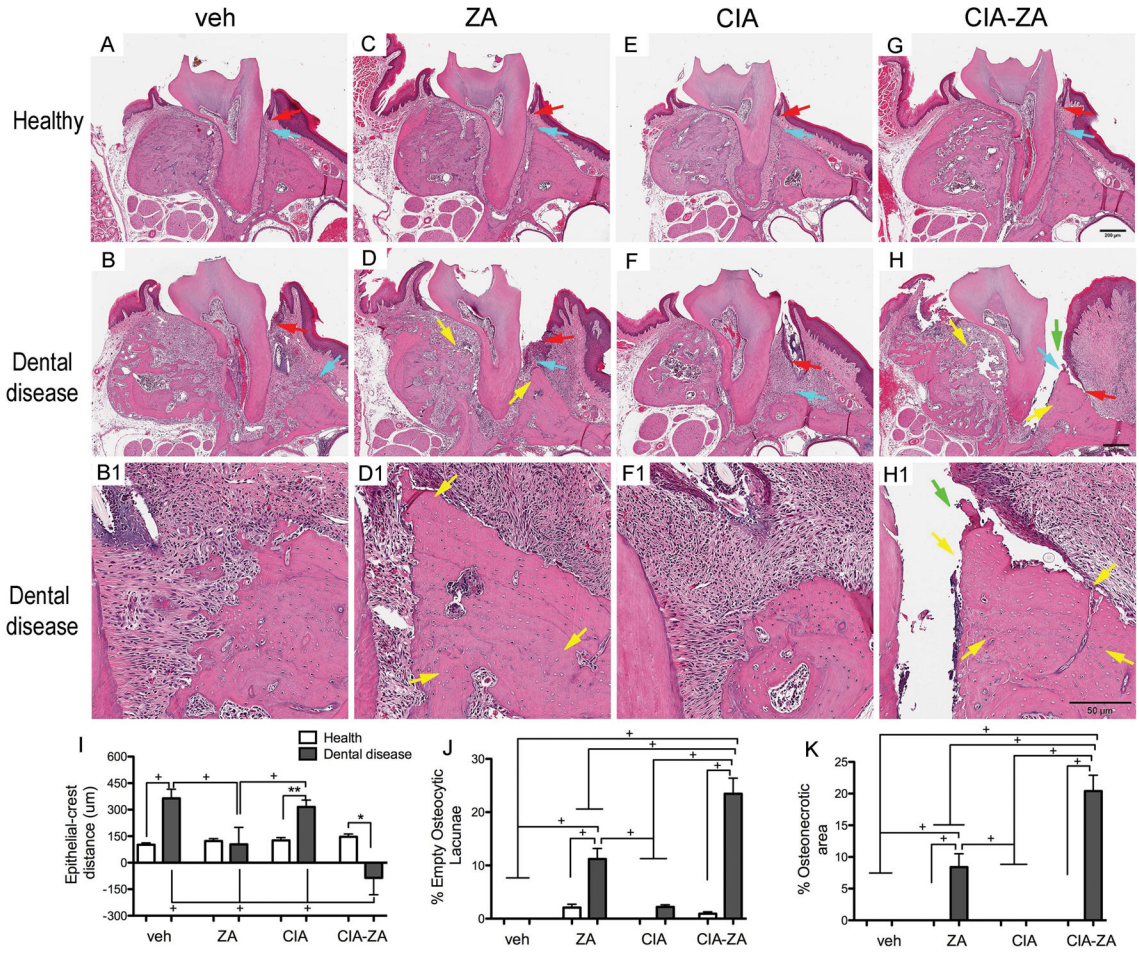

Figure 3. Representative H&E-stained images from maxilla of all groups and quantification of the histologic findings

(A, C, E and G) Healthy and (B, D, F and H) diseased site of vehicle, ZA, CIA and CIA-ZA mice. Original magnification, x5. (B1, D1, F1 and H1) Histologic appearance of periodontal and alveolar crest area of maxillae in magnified views of the diseased site. Original magnification, x10. Red arrows point to marginal gingival epithelium, turquoise arrows to alveolar crest, yellow arrows to osteonecrotic areas, and green arrows to areas of bone exposure. (I–K) Quantification of the histologic findings: The shortest epithelial-crest distance, percentage of osteocytic lacunae and percentage of areas of osteonecrosis were measure, respectively. + Statistically significant different from indicated groups, $p < 0.0001$. ** Statistically significant different from indicated groups, $p < 0.001$. * Statistically significant different from indicated groups, $p < 0.05$. Differences among groups were calculated by two-way ANOVA and between groups by Student's t test. Data represent the mean ± SEM.

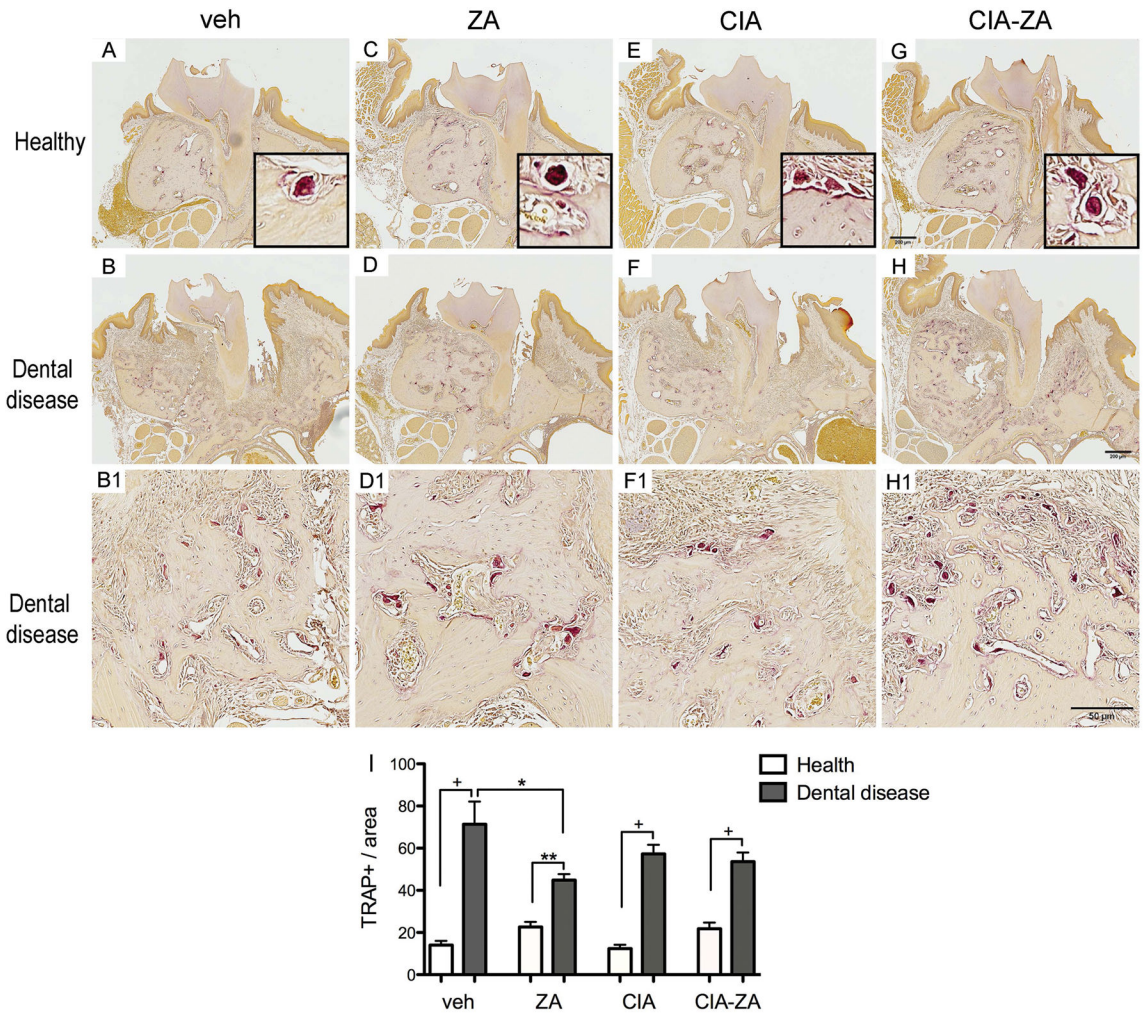

Figure 4. Representative sections of the maxilla stained for TRAP+ cells

(A, C, E and G) Healthy site of vehicle, ZA, CIA and CIA-ZA, respectively. Original magnification, x5. Insets are magnified views of individual TRAP+ cells. Original Magnification, x20. (B, D, F and H) Diseased site at the end of the treatment. (B1, D1, F1 and H1) Magnified views of the diseased site in vehicle, ZA, CIA and CIA-ZA, respectively. Original magnification, x10. (I) Quantification of TRAP + cell number in all mice and groups. (n = 6 mice per group). + Statistically significant different from indicated groups, $p < 0.0001$. ** Statistically significant different from indicated groups, $p < 0.001$. * Statistically significant different from indicated groups, $p < 0.05$. Differences among groups were calculated by two-way ANOVA and between groups by Student's t test. Data represent the mean ± SEM.

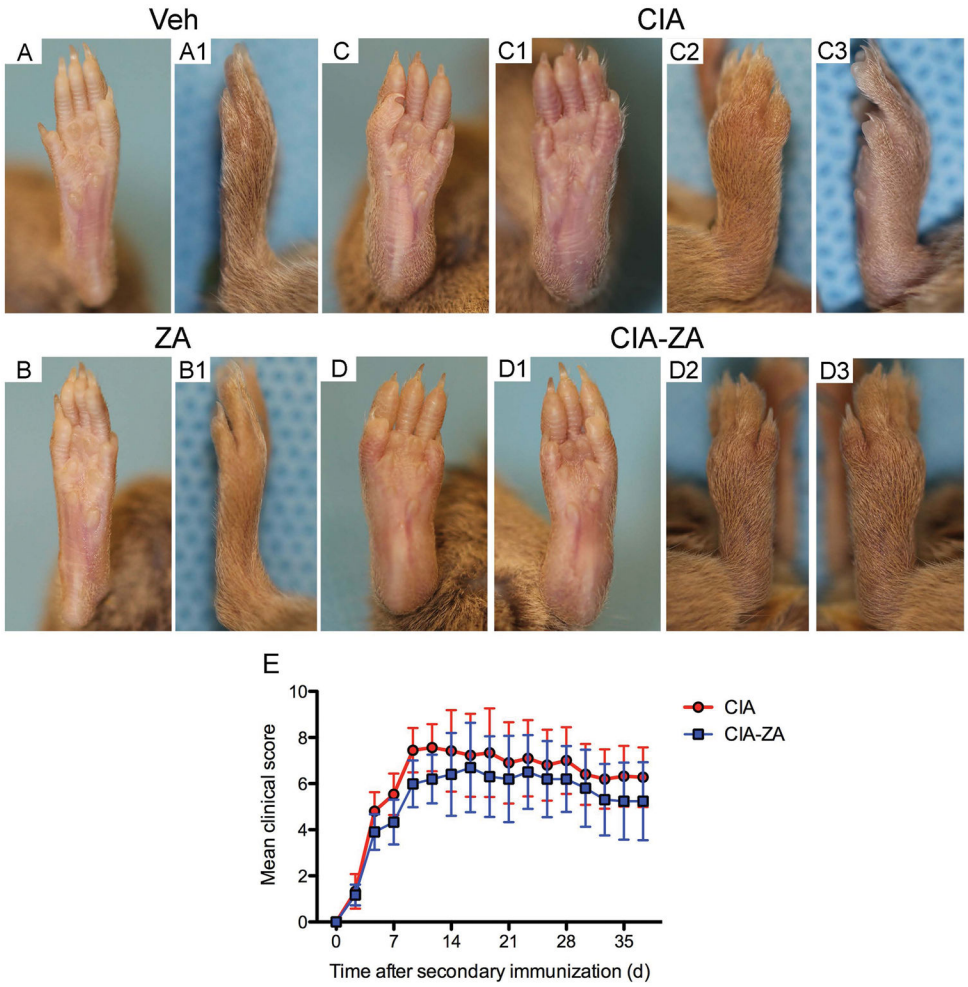

Figure 5. Clinical course of RA

Clinical evaluation of the paws were performed and scored for arthritis every other day from day 21 after the first immunization until the time of euthanasia. (A, A1, B, B1) Frontal and lateral views of vehicle and ZA treated mice. (C, C1, C2, C3, D, D1, D2, D3) Frontal and lateral views of CIA and CIA-ZA treated mice. All fingers of forepaws, hind paws, wrists and ankles were totaled for each mouse (maximum possible score of 12 for each mouse). (E) Mean and standard deviation of the clinical assessment until day 35 after second immunization.

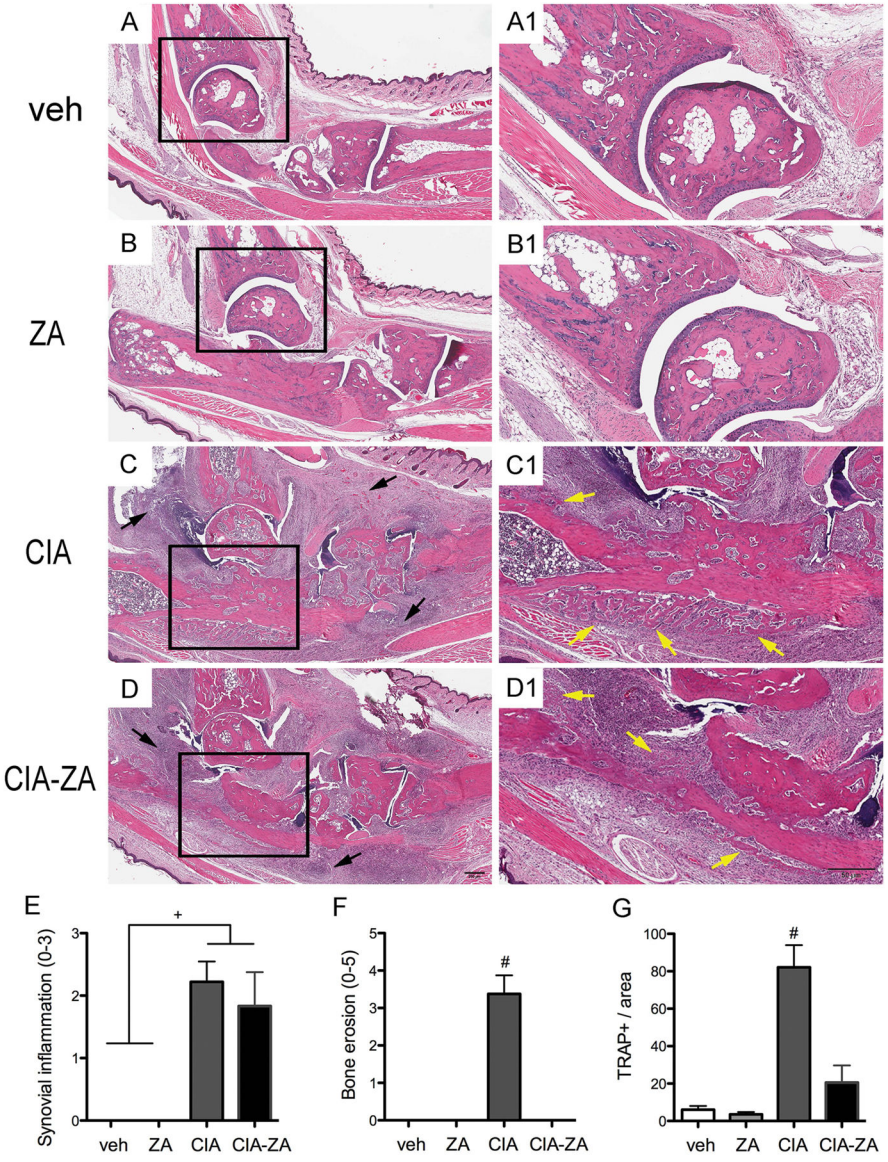

Figure 6. Histopathologic effects of ZA treatment in the hind paws and TRAP + cells staining

Total ankle joints were isolated for histopathologic analysis (n = 6 mice per group). (A–D) Sagittal sections of the vehicle, ZA, CIA and CIA-ZA, respectively. Original magnification, x5. (A1–D1) Magnified views of the area represented by the black squares. Original magnification, x10. Black arrows point to inflammatory infiltration. Yellow arrows point to periosteal bone formation. (E–F) Quantification of the histopathologic findings in the ankle: Synovial inflammation, and bone erosions were measured in all groups at the end of the treatment. (G) Quantification of the TRAP+ cells number in all mice and groups. # Statistically significant different compared to all the other groups, $p < 0.0001$. + Statistically significant different from indicated groups, $p < 0.0001$. Differences among groups were calculated by two-way ANOVA and between groups by Student's t test. Data represent the mean ± SEM.

Table 1

Summary of radiographic and histologic findings on various groups.

Group	Total hemi-mandible & hemi-maxillae	Healthy (%)	Diseased (%)	Osteonecrosis (%)	Bone Exposure (%)
Vehicle	24	12 (50) *	12 (50) *	0 $ (0) * (0) #	0 @ (0) * (0) # (0) +
ZA	24	10 (41.7) *	14 (58.3) *	9 (37.5) * (64.3) #	3 (12.5) * (21.4) # (33.3) +
CIA	24	9 (37.5) *	15 (62.5) *	0 $ (0) * (0) #	0 @ (0) * (0) # (0) +
CIA-ZA	24	9 (37.5) *	15 (62.5) *	13 (54.2) * (86.7) #	7 (29.2) * (46.7) # (53.4) +

*% of total hemimaxillae and hemimandible;

#% of diseased hemimaxillae and hemimandible;

+% of hemimaxillae and hemimandible with osteonecrosis;

$Statistically significantly different, $p < 0.001$ compared to ZA and CIA-ZA;

@Statistically significantly different, $p < 0.001$ compared to CIA-ZA;

J Bone Miner Res. Author manuscript; available in PMC 2017 August 01.